

# Mott transition from a diluted exciton gas to a dense electron-hole plasma in a single V-shaped quantum wire

T. Guillet,<sup>\*</sup> R. Grousson, V. Voliotis,<sup>†</sup> and M. Menant

*Groupe de Physique des Solides, CNRS,  
Universités Pierre et Marie Curie et Denis Diderot,  
2 place Jussieu, F-75251 Paris Cedex 05, France*

X.L. Wang<sup>‡</sup> and M. Ogura

*Photonics Research Institute, National Institute of  
Advanced Industrial Science and Technology (AIST),  
Tsukuba Central 2, Tsukuba 305-8568, Japan  
and CREST, Japan Science and Technology Corporation (JST),  
4-1-8 Honcho, Kawaguchi 332-0012, Japan*

(Dated: May 21, 2019)

## Abstract

We report on the study of many-body interactions in a single high quality V-shaped quantum wire by means of continuous and time-resolved microphotoluminescence. The transition from a weakly interacting exciton gas when the carrier density  $n$  is less than  $10^5 \text{ cm}^{-1}$  (i.e.  $na_X < 0.1$ , with  $a_X$  the exciton Bohr radius), to a dense electron-hole plasma ( $n > 10^6 \text{ cm}^{-1}$ , i.e.  $na_X > 1$ ) is systematically followed in the system as the carrier density is increased. We show that this transition occurs gradually : the free carriers first coexist with excitons for  $na_X > 0.1$ , then the electron-hole plasma becomes degenerate at  $na_X = 0.8$ . We also show that the non-linear effects are strongly related to the kind of disorder and localization properties in the structure especially in the low density regime.

PACS numbers: 71.35.Lk; 71.35.Ee; 78.55.Cr; 78.67.Lt

---

<sup>\*</sup>Also at Département de Physique, Ecole Polytechnique Fédérale de Lausanne, Switzerland; Electronic address: guillet@gps.jussieu.fr

<sup>†</sup>Also at Université Evry-Val d'Essonne, France

<sup>‡</sup>Also at Department of Electrical Engineering, Yale University, USA

## I. INTRODUCTION

Non-linear effects in one-dimensional (1D) systems have been recently the subject of many theoretical as well as experimental investigations, due to the potential applications for optoelectronic devices and especially for incorporating low dimensional heterostructures, like quantum wires, in lasers.

It has been predicted that due to the suppression of the 1D singularity in the density of states because of the important Coulomb correlations in one dimension, the exciton transition has an enhanced oscillator strength and stability compared to quantum wells [1, 2]. Many questions arise then: up to what carrier densities is the exciton stable ? When does the Mott transition occur in a quantum wire (QWR) and what is the origin of the emission line in 1D systems when the carrier density is increased ? There is a controversy in theory on this point, especially for the critical carrier density at the Mott transition [3, 4, 5]. A typical predicted feature of a Mott transition in optical experiments is the existence of gain in the absorption spectrum at some energy range. But in some studies excitonic lasing is told to be possible in one-dimensional structures. Rossi et al [2] found optical gain at a carrier density of  $4 \cdot 10^6 \text{ cm}^{-1}$  while the calculated Mott transition occurs at  $8 \cdot 10^5 \text{ cm}^{-1}$ . So, the authors predict that lasing due to electron-hole pairs may occur in a QWR. Piermarrochi et al [4] predict that optical gain occurs at  $10^5 \text{ cm}^{-1}$ , below the Mott transition, while Das Sarma et al [3] found no gain at any carrier density. However in photoluminescence experiments where the emission is observed, there is no signature of the presence of gain in the structure, and it is more difficult to evidence a Mott transition. The existence of the Mott transition is still under debate, depending also on the definition itself. In many-body theories treating the Coulomb correlations between free carriers, the transition occurs when an electron and a hole cannot form a bound pair and the obtained critical density is  $na_X \approx 0.1 - 1$  [2, 3, 4, 5] where  $n$  is the carrier density and  $a_X$  is the exciton Bohr radius in the s

ystem. However in many-body theories treating Coulomb interactions between excitons, the transition occurs as soon as carriers (electron or hole) can be exchanged between two excitons. Then the Mott criterion is very much weakened, by a factor 100 in two-dimensionnal systems [6].

Experimentally, optical non-linearities under high pump excitation have been studied previously by other groups in less confining QWRs [7, 8]. Band filling has been evidenced

and according to a theoretical modelisation of the results, band gap renormalization has been observed. Ambigapathy et al [9] have studied dynamics of excitons under high density regime. The authors conclude that the band gap renormalization is exactly compensating the exciton binding energy and the exciton remains the stable excitation under very high pump power ( $n = 3 \cdot 10^6 \text{ cm}^{-1}$ ,  $na_X = 3$ ). The high density dynamics is also of crucial importance in the understanding of the lasing mechanism in QWR structures [10]. Recently excitonic lasing in QWRs has been reported [11, 12, 13], based on the observation that the emission energy remains nearly constant within the inhomogeneously broadened photoluminescence line. We believe that this experimental evidence is not a sufficient criterion since at the high carrier density for which lasing is obtained, an electron-hole plasma (EHP) is formed in the wire and emits at the same energy. Therefore excitonic lasing in 1D structures is still an open question to our point of view.

We have performed systematic studies of continuous and time resolved photoluminescence of a single quantum wire, as a function of carrier density, by means of optical imaging spectroscopy. We show that the different non-linearities observed, depend strongly on the kind of local disorder in the wire especially in the low density limit. As pump power is increased the exciton emission line gets broader but remains at a constant energy position within a few  $meV$ . No distinct features appear in the spectra, for instance a line that could be attributed to the EHP emission. However we show that a gradual transition in the nature of excitations has occurred in the system. Indeed, the time-resolved photoluminescence experiments in the high density regime reveal that the emission is due to the formation of an EHP and not to excitons.

## II. DISORDER EFFECTS IN V-SHAPED QWRs

The studied samples are 5 nm thick V-shaped GaAs/Ga<sub>0.57</sub>Al<sub>0.43</sub>As QWRs grown by flow rate modulation epitaxy on a 4  $\mu\text{m}$  pitched V-grooved GaAs substrate [14]. These samples are very high quality structures with strong confinement (the energy spacing between the first and second subbands e1h1 and e2h2 is 60  $meV$ ) and showing specific 1D properties, like large optical anisotropy due to 1D valence band mixing. The localization of excitons in these QWRs has been studied by microphotoluminescence ( $\mu$ -PL). The low temperature  $\mu$ -PL setup is composed of a microscope objective with a large numerical aperture (0.6)

which is fixed on a three axis piezoelectric stage. This allows to scan images along a single QWR. The spatial resolution of the set-up is  $1\ \mu m$ , the spectral resolution is  $40\ \mu eV$  and the temporal resolution is  $20\ ps$ . Excitation wavelength was always adjusted with a Ti-Sa or a dye laser in order to create carriers only in the wire. This is important for the correct calibration of the carrier density in the wire. Details of the set-up can be found elsewhere [16, 17].

Our former studies have shown that at low temperatures, the optical properties of excitons in the previous generation of QWRs are governed by localization effects leading to a discrete spectrum of states [16]. Monolayer thickness fluctuations along the growth axis occur, leading to the formation of local potential minima with a mean size of  $50\ nm$  along the wire axis. Optical imaging spectroscopy has allowed to characterize the local confining potential along the wire axis and to relate the local disorder to the optical properties [17]. Excitons are localized in such quantum boxes and at very low pump power, the emission is composed of very sharp lines corresponding to the emission of the lowest lying exciton states in each box. The energy spectrum is discrete and the exciton dynamical properties are those of a zero-dimensional (0D) system [16]. We say then that the QWRs are in a 0D regime. When the density of excitons created in average is increased, different effects appear depending on the size of the box along the wire axis. The density threshold for non-linear effects being one exciton per box, the interaction between excitons will be weak if they are trapped in different boxes and more effective when trapped in the same box. Two different behaviours have been reported [18, 19]: biexciton formation or Auger scattering depending on the size of the box. As the density is further increased, state filling effects occur with an important broadening of the emission band due to exciton-exciton or exciton-free carriers interactions.

Recent progresses in the growth techniques allowed to further reduce the heterointerfaces roughness of the QWR [20]. In this new generation of QWRs, the optical imaging spectroscopy shows that the thickness fluctuations on the (001) facet occur every  $5\ \mu m$  while the other heterointerfaces (311) and (111) present monolayer fluctuations from  $0.5$  to  $2\ \mu m$  [17]. A typical scanning image of a single QWR is shown in figure 1. Each bright spot corresponds to the emission from the lowest lying level in local potential minima along the wire axis. The linear density of the emitting sites is about 1 per  $\mu m$  and the mean potential minimum length is  $400\ nm$  as it is obtained after statistical analysis [17]. Sometimes the emitting region can reach  $3\ \mu m$  on one wire, for example at the position indicated by a white

arrow on the image. In such a very long island, the localization length is much larger than the thermal de Broglie wavelength of the excitons, and the excitonic states form a quasi-continuum of states leading to 1D behaviour of the system. These samples are told to be in a 1D regime. The emission spectrum is then composed of a single homogeneously broadened line as it shown on figure 1. Another evidence for the 1D character of the system is that the radiative lifetime as a function of temperature shows the characteristic  $\sqrt{T}$  dependence [17]. This behaviour reflects the  $1/\sqrt{E}$  1D local density of states.

### III. MANY-BODY EFFECTS IN 1D REGIME QWRS

We have studied continuous and time-resolved PL in different carrier density regimes in the 1D regime QWRs described above. Three density limits can be distinguished if we compare the average distance between excitons  $1/n$ , to the exciton Bohr radius  $a_X$  which is equal to 70 Å in our structure for a binding energy of 20 *meV* [21]. When the density of excitons  $n$  is very low then  $na_X \ll 1$  and the excitons form a weakly interacting gas, we say in that case to be in a “dilute” regime. On the opposite, the “dense” regime corresponds to very high carrier density where  $na_X \gg 1$  and in this case we expect a dense EHP to be formed. Inbetween, there is also an “intermediate” regime for which a Mott transition should occur in the system.

Figure 2 represents typical  $\mu$ -PL spectra under continuous excitation of a very long island (about 3  $\mu m$ ) as a function of carrier density in the low density regime. Excitation energy is at 1.75 *eV* in the e3h3 transition of the QWR. At very low pump power ( $P = 0.1 \text{ W.cm}^{-2}$ ) one main  $\mu$ -PL peak appears, labelled A on the figure, corresponding to the emission of the lowest lying exciton level in this island. As a matter of fact, two other peaks labelled B, and C appear in the spectrum due to the presence of neighbouring islands that are excited by the laser spot, as it has been shown by the scanning images of the QWR (figure 1). However, their intensity is less than peak A intensity by a factor 10 and 30 respectively. As the pump power is increased up to  $5.4 \cdot 10^3 \text{ W.cm}^{-2}$ , there is a slight blue shift of line A by 0.2 *meV* and a new line appears in the spectrum corresponding to the formation of a biexciton (labelled  $A_2$ ). The biexciton binding energy can be deduced from the spectrum and is equal to 1.5 *meV* which is in very good agreement with theoretical calculations [22] and similar to other experimental observations [23]. The intensity of peak A has a linear behaviour with

pump power and saturates above  $10^4 \text{ W.cm}^{-2}$  while peak A<sub>2</sub> has a super-linear behaviour as expected for biexciton. The total integrated intensity of the luminescence line is linear with pump power. At the maximum pump power the lines get broader and a broad background grows up. This background can be attributed to the radiative recombination processes which are assisted by Coulomb collisions between excitons or excitons and free carriers. Similar observations have been reported by Vouilloz et al [24].

The calibration of the carrier density created in the QWR is made from the data of saturation of exciton and biexciton emission intensities in the 0D regime QWRs [25]. We estimate that for a CW pump excitation at 1.75 eV,  $400 \text{ W.cm}^{-2}$  correspond to 1 exciton per  $\mu\text{m}$ , i.e. a carrier density of  $10^4 \text{ cm}^{-1}$  and to a number  $na_X$  equal to  $7 \cdot 10^{-3}$ . This calibration has been used for the estimation of the carrier density presented in all the following experiments.

As the upper limit of the dilute regime is reached ( $n = 10^5 \text{ cm}^{-1}$ , i.e.  $na_X \approx 0.1$ ) the lines associated to exciton and biexciton transitions are still clearly marked showing that these are the stable elementary excitations in the system.

The intermediate ( $0.1 < na_X < 1$ ) and dense regime ( $na_X > 1$ ) are represented in figure 3. In order to study the dense regime ( $na_X > 1$ ) pulsed laser excitation has been used to provide very high carrier concentration in the wire up to  $n \approx 10^7 \text{ cm}^{-1}$ , i.e.  $na_X = 20$ . For ( $0.1 < na_X < 1$ ) the spectra obtained under continuous and pulsed excitation are similar. The peak labelled A corresponds to the main exciton line of a  $2 \mu\text{m}$  long island. The other peaks labelled B, C, and D correspond as usual to neighbouring islands excited by the tails of the laser spot. A<sub>2</sub> is the biexciton emission line.

Let us first focus on the intermediate regime. A qualitative change of the spectra is observed above  $na_X = 0.1$ . The exciton and biexciton lines are broadened, they shift towards higher energies by 2 meV and finally disappear. The shift of the lines is a signature of the many-body interactions : it corresponds to a competition between the band gap renormalization (BGR) occurring as we fill the carriers subbands and the screening of the exciton binding energy. The sum of both effects give rise to small energy shifts in 1D structures, only a few meV, moreover an almost exact cancellation of these effects is predicted [2, 3]. The fast growing up of the broad background is attributed to the presence of free electron-holes pairs. It progressively overcomes the excitonic transition as the excitation power is increased.

Another experimental evidence of the presence of free carriers in the intermediate regime is that there is a spatial diffusion of the carriers. Indeed we have measured the spatial distribution of the emission as a function of the carrier density by the optical imaging setup. Its spatial resolution is  $1.5 \mu m$ , limited by the imaging spectrometer, and is larger than the diameter of the laser excitation spot ( $0.8 \mu m$ ). The recorded  $\mu$ -PL spatial profile can be very easily fitted by a Gaussian curve whose width is reported in figure 4 as a function of carrier density. For  $na_X < 0.1$ , the spatial distribution width is limited by our experimental resolution. Above this density, the emitting region gets larger, showing that diffusion of carriers takes place along the wire axis before radiative recombination. We have checked that in the low density regime, excitons do not diffuse even up to  $70 K$  [25], because the exciton-exciton scattering mechanism is less efficient than interaction with free carriers [26]. Here, the observed diffusion for a carrier density above  $10^5 cm^{-1}$  is due to the presence of free carriers that are responsible for the scattering with excitons. The temperature of the carriers deduced from the high energy tail of the PL spectrum is  $40 K$  at the highest density, so that the diffusion isn't thermally activated and is due to collisions between carriers. The density where this process occurs is  $n \approx 10^5 cm^{-1}$ , i.e.  $na_X \approx 0.1$  and corresponds to the qualitative change observed in the luminescence spectrum (figure 3) [27]. Both the diffusion of the carriers and the spectral broadening of the exciton and biexciton transitions show that free electrons and holes coexist with excitons and progressively overcome them above  $na_X = 0.1$ .

The  $\mu$ -PL spectra reported on Figure 3 also present the dense regime. Above  $na_X = 1$ , higher order subbands (e2, h2, h3, ...) are also filled : the optically allowed transitions e1h5 and e2h2 appear in the PL spectra at the same position as in the PLE spectra. It is worth noticing that the PL line centered at the exciton energy position does not shift significantly up to the highest excitation power. This is consistent with previous experimental findings [8, 9] and reflects the almost cancellation of BGR and screening of the exciton binding energy in 1D systems.

The temporal evolution of the  $\mu$ -PL provides a more detailed understanding of the system and is shown on figure 5 at the highest carrier density, corresponding to the top curve of Fig. 3 ( $n = 2.5 \cdot 10^7 cm^{-1}$ , i.e.  $na_X = 20$ , at  $t = 0$ ). The detection energy is set at different positions labelled  $E_0$ ,  $E_1$ ,  $E_2$  on the figure 3. For the three curves, we first observe a very fast rising time ( $0 < t < 50 ps$ ), then a slowing down during  $200 ps$  which corresponds probably to the

setting up of the quasi-equilibrium in the system. Then a characteristic saturation plateau is observed which persists longer as the detection energy is lower in the band. The PL intensity at the plateau is the same within 20% at the three detection energies, and a slight increase at  $E_1$  and  $E_2$  is observed, which is not explained at the moment. The temporal decay is different for the three curves. It is non-exponential for the case of higher detection energies ( $E_1$  and  $E_2$ ) and reflects the complicated carrier dynamics at high energy. When detecting on the band edge energy  $E_0$ , the decay is nearly mono-exponential with a characteristic time corresponding to the exciton radiative lifetime (about 300 ps) as confirmed by the low density temporal decay also shown on figure 5.

The dependence of the saturation plateaux with detection energy is characteristic of an EHP emission and not of exciton luminescence. Indeed if this were the case, due to the conservation of the k-selection rule, only  $k = 0$  excitons could recombine and then the saturation should be independent on the energy position in the line. On the contrary, we may qualitatively interpret the PL temporal evolutions as follows : at  $t = 0$ , as the laser pulse excites the system, the carrier density is about  $2.5 \cdot 10^7 \text{ cm}^{-3}$  ( $na_X \approx 20$ ). An EHP out of equilibrium is likely formed at this high density regime. Electron and hole subbands are filled over hundreds of meV up to the chemical potentials  $\mu_{e,h}$ , and luminescence comes from the vertical transitions between electrons and holes of the different subbands. In a simplified single electron-hole band scheme described by only one potential  $\mu$ , the carrier density is progressively reduced as recombination takes place, then  $\mu$  decreases in energy and the subband empties. When  $\mu$  is larger than the detection energy  $E$  by an amount larger than  $kT$ , the occupancy factor at energy  $E$  is unity and the luminescence intensity saturates. When  $\mu = E$ , the occupancy factor decreases and the luminescence decreases rapidly as well. When  $E - \mu \gg kT$ , the occupation factor at energy  $E$  is a Maxwell-Boltzmann distribution and the carriers at energy  $E$  are at thermal equilibrium with the band-edge. The carrier density corresponding to  $\mu = E_0$  is actually the density above which electron and hole subbands are filled and the electron-hole plasma ends to be degenerate. The whole process is schematically drawn on top of figure 5. The time-resolved PL reflects in fact the chemical potential temporal evolution and can be related to the carrier density. In a first order approximation we may assume that the entire population decays with the same lifetime (the exciton radiative lifetime). The carrier density we found in this way, correspond

ing to  $\mu = E_0$  is about  $n \approx 1.2 \cdot 10^6 \text{ cm}^{-1}$ , i.e.  $na_X \approx 0.8$ . This threshold density corresponds to the transition to a degenerate EHP, i.e. to the filling of the first electron and hole subbands.

However in order to have a full description of the chemical potential evolution as a function of  $n$  in the degenerate EHP, one would have to study the temporal decay of the whole PL line and know more precisely the population decay. This would also allow to measure the precise shape of the plateaux, which depends on the selection rules governing the recombination process (conservation of energy, momentum, or both of them) and the renormalization of electron and hole energy dispersion as a function of the density.

In ref. [9] where similar results have been obtained, the authors present the time decay of the *integrated* PL in order to analyse the radiative decay of the carriers. Their main conclusion is that the recombination is dominated by “excitonic correlations” even at high density ( $3 \cdot 10^6 \text{ cm}^{-1}$ ) since the decay is mono-exponential with the characteristic exciton lifetime. We show here the energy- and time-resolved PL provides a more complete understanding of the dynamics and proves that a fully degenerate EHP is formed at high density, excluding the presence of excitons.

#### IV. CONCLUSION

We have monitored the apparition of free carriers as well as the degeneracy of the EHP in a QWR by an extended study of their spectroscopy and dynamics, coupled to a local study relieving the inhomogeneous broadening of the transitions. Our results clearly show that the energy position of the emission line is not a sufficient criterion in order to determine the nature of the excitations in the system, as it was previously argued concerning the lasing mechanism in QWR lasers [11, 12, 13]. In the low density regime the situation depends on the localization regime. In 0D regime QWRs with a localization length of the order of  $50 \text{ nm}$ , a competition between Auger effects and biexciton formation has been observed. But in 1D regime QWRs, in which each island is extended over  $0.5$  to  $3 \text{ }\mu\text{m}$  and can be considered as a small portion of really 1D QWR, excitons are stable until  $na_X \approx 1$ , and they coexist with free charges above  $na_X \approx 0.1$ . For  $na_X > 0.01$ , biexcitons are formed and the slight shifts of the exciton line are a signature of Coulomb interactions between excitons. Above  $na_X = 0.1$  ( $10^5 \text{ cm}^{-1}$ ) free electrons and holes coexist with excitons, leading to a

broad spectral background and the diffusion of carriers along the wire axis. In the dense regime ( $na_X > 1$ ,  $n > 10^6 \text{ cm}^{-1}$ ) the saturation observed is the signature of a degenerate EHP luminescence excluding the possibility of exciton formation and reflects the temporal evolution of the chemical potential. Our results are in quite good agreement with recent theoretical calculations which predict that no new emission line attributed to the EHP should appear in the emission spectrum. This is due to the fact that the energy shifts associated to the screening of the exciton binding and to BGR occurring at high density are small (few  $\text{meV}$ ) in QWRs because of the compensation of these two effects.

- 
- [1] T. Ogawa, T. Takagahara, Phys. Rev. B **43**, 14325 (1991)
  - [2] F. Rossi, E. Molinari, Phys. Rev. Lett. **76**, 3642 (1996)
  - [3] S. Das Sarma, D.W. Wang, Phys. Rev. Lett. **84**, 2010 (2000); Phys. Rev. B **64**, 195313 (2001)
  - [4] C. Piermarocchi, F. Tassone, Phys. Rev. B **63**, 245308 (2001)
  - [5] M. Stopa, Phys. Rev. B **63**, 195312 (2001) P.B. Littlewood, K.W. West, B.S. Dennis, Solid State Commun. **120**, 423 (2001)
  - [6] M. Combescot, C. Tanguy, EuroPhys. Lett. **55**, 390 (2001)
  - [7] C. Gréus, A. Forchel, R. Spiegel, F. Faller, S. Benner, H. Haug, Europhys. Lett. **34**, 213 (1996)
  - [8] R. Cingolani, R. Rinaldi, M. Ferrara, G.C. La Rocca, H. Lage, D. Heitmann, K.H. Ploog, H. Kalt, Phys. Rev. B **48**, 14331 (1993)
  - [9] R. Ambigapathy, I. Bar-Joseph, D.Y. Oberli, S. Haacke, M.J. Brasil, F. Reinhardt, E. Kapon, B. Deveaud, Phys. Rev. Lett. **78**, 3579 (1997)
  - [10] T.G. Kim, X.L. Wang, R. Kaji, M. Ogura, Physica E **7**, 508 (2000)
  - [11] W. Weigsheider, L.N. Pfeiffer, M.M. Dignam, A. Pinczuk, K.W. West, S.L. McCall, R. Hull, Phys. Rev. Lett. **71**, 4071 (1993)
  - [12] L. Sirigu, D.Y. Oberli, L. Degiorgi, A. Rudra, and E. Kapon, Phys. Rev. B **61**, R10575 (2000)
  - [13] J. Rubio, L. Pfeiffer, M.H. Szymanska, A. Pinczuk, S. He, H.U. Baranger, P.B. Littlewood, K.W. West, B.S. Dennis, Solid State Commun **120**, 423 (2001)
  - [14] X.L. Wang, M. Ogura, H. Matsuhata, Appl. Phys. Lett. **67**, 804 (1995); J. Crystal Growth **195**, 586 (1998)
  - [15] J. Bellessa, V. Voliotis, R. Grousson, X.L. Wang, M. Ogura, H. Matsuhata, Appl. Phys. Lett.

- 71**, 2481 (1997)
- [16] J. Bellessa, V. Voliotis, R. Grousson, X.L. Wang, M. Ogura, H. Matsuhata, Phys. Rev. B **58**, 9933 (1998)
  - [17] T. Guillet, V. Voliotis, R. Grousson, M. Menant, X.L. Wang, M. Ogura, submitted to Phys. Rev. B under Reference BY8100
  - [18] Q. Wu, R.D. Grober, D. Gammon, D.S. Katzer, Phys. Rev. B **62**, 13022 (2000)
  - [19] J. Bellessa, V. Voliotis, T. Guillet, D. Roditchev, R. Grousson, X.L. Wang, M. Ogura, Eur. Phys. J. B **21**, 499 (2001)
  - [20] X.L. Wang, M. Ogura, J. Crystal Growth **221**, 556 (2000)
  - [21] M. Combescot, T. Guillet, to be published.
  - [22] L. Banyai, I. Galbraith, C. Ell, H. Haug, Phys. Rev. B **36**, 6099 (1987); by taking our wire size, a ratio of 1 to 10 is found between the biexciton and the exciton binding energies.
  - [23] A. Crottini, J.L. Staehli, B. Deveaud, X.L. Wang, M. Ogura, Phys. Stat. Sol. (b) **221**, 277 (2000)
  - [24] F. Vouilloz, D.Y. Oberli, F. Lelarge, B. Dwir, E. Kapon, Solid State Comm. **108**, 945 (1998)
  - [25] T. Guillet, *Thèse de l'Université Pierre et Marie Curie* (Paris, 2002)
  - [26] A. Honold, L. Schulteis, J. Kuhl, C.W. Tu, Phys. Rev. B **40**, 6442 (1989)
  - [27] The estimated carrier densities in the dense regime have been corrected by the diffusion of carriers, especially in fig. 3.

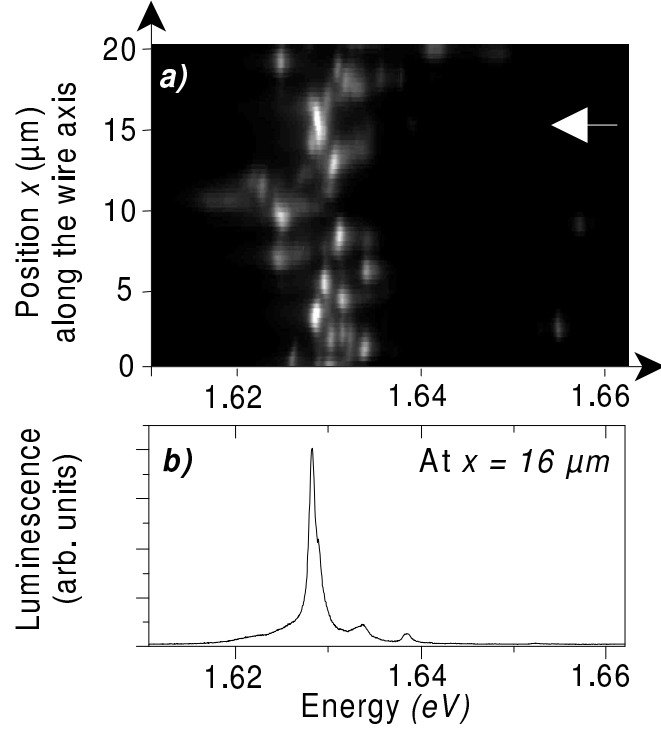


FIG. 1: a) Scanning optical image of a single QWR. The  $\mu$ -PL intensity is represented in gray levels. b) Typical  $\mu$ -PL spectrum extracted from the image at the position indicated by a white arrow.

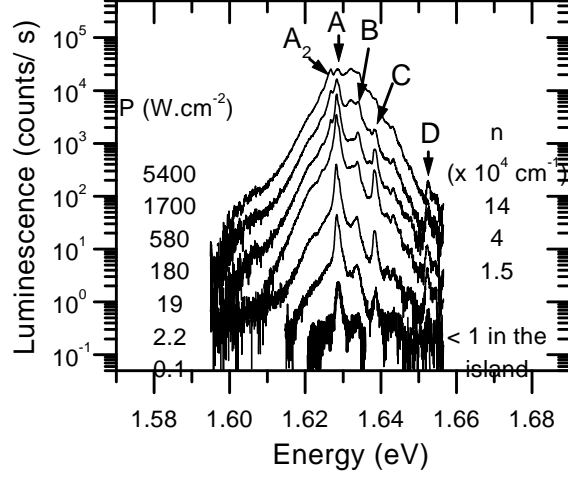


FIG. 2:  $\mu$ -PL spectra as a function of the pump power at 11 K, under continuous excitation at 1.75 eV in the e3h3 transition of the wire. Peaks A and A<sub>2</sub> correspond respectively to the exciton and biexciton transitions of the considered island which is extended over 3  $\mu$ m, while B, C and D are associated to neighboring islands. The carrier densities are indicated for the 3 highest excitation powers.

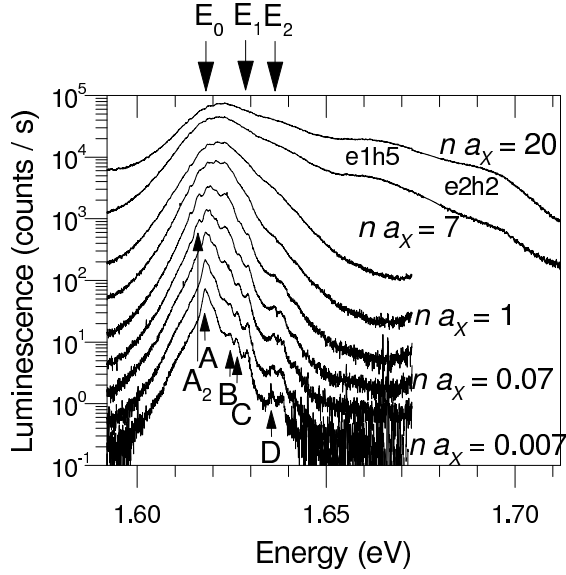


FIG. 3:  $\mu$ -PL as a function of carrier density under laser pulsed excitation at 11 K, in an extended island similar to Figure 2. The excitation energy is 1.77 eV in the e4h4 transition of the wire. The spectra correspond to carrier densities  $na_x$  of 0.007, 0.02, 0.07, 0.2, 0.5, 1, 3, 7 and 20 from bottom to top.

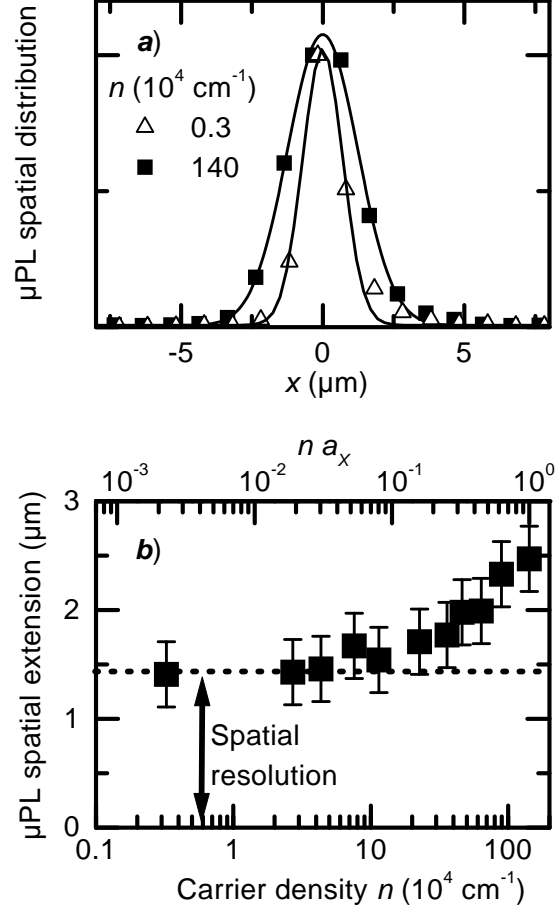


FIG. 4: a) Spatial profile of the luminescence emitted by an extended island under continuous excitation at  $x = 0$ , for two carrier densities at  $T = 11 \text{ K}$ . b) Width of the fitting Gaussian curve is represented as a function of carrier density.

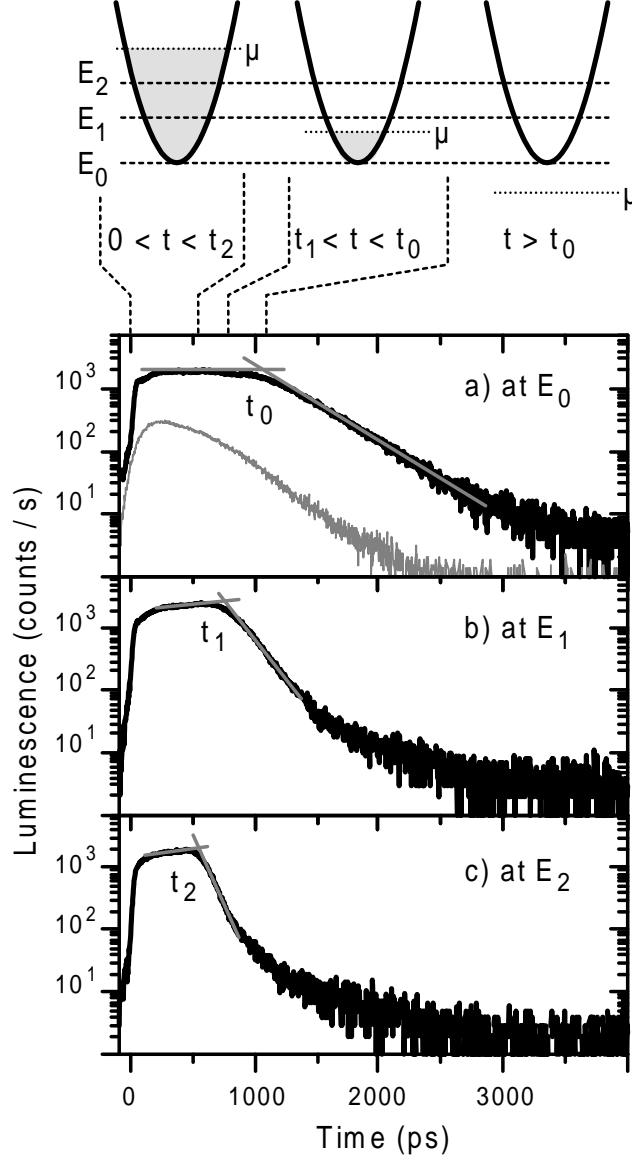


FIG. 5: Temporal evolution of the  $\mu$ -PL at high power excitation ( $P = 8 \cdot 10^4 \text{ W.cm}^{-2}$ ) detected at different energy positions in the line ( $E_0 = 1.619 \text{ eV}$ ,  $E_1 = 1.629 \text{ eV}$ ,  $E_2 = 1.639 \text{ eV}$ ) in the experiment presented on figure 3. The temporal evolution of the chemical potential is schematically drawn on top in a simplified single electron-hole band picture. The temporal evolution of the  $\mu$ -PL at  $E_0$  at a lower pump power ( $P = 8 \cdot 10^3 \text{ W.cm}^{-2}$ ) is presented in gray line in (a).